Mol Genet Genomics (2002) 267: 721–729
DOI 10.1007/s00438-002-0705-2

ORIGINAL PAPER

M.A. Schembri · D.W. Ussery · C. Workman
H. Hasman · P. Klemm

DNA microarray analysis of *fim* mutations in *Escherichia coli*

Received: 25 February 2002 / Accepted: 22 May 2002 / Published online: 21 June 2002

Abstract Bacterial adhesion is often mediated by complex polymeric surface structures referred to as fimbriae. Type 1 fimbriae of *Escherichia coli* represent the archetypical and best characterised fimbrial system. These adhesive organelles mediate binding to D-mannose and are directly associated with virulence in the urinary tract. A typical type 1 fimbriated bacterium has up to 500 fimbriae on its surface, with each fimbria consisting of ~1000 individual subunits. This equates to approximately 8% of the total cellular protein and is potentially a significant resource drain for the cell. Here we have used DNA microarray analysis to examine the molecular events involved in response to fimbrial gene expression in *E. coli* K-12. Observed differential expression levels of the *fim* genes were in good agreement with our current knowledge of the stoichiometry of type 1 fimbriae. Changes in *fim* expression correlated directly with alterations in colony morphology. Deletion of the entire *fim* gene cluster resulted in the converse expression of another surface protein Antigen 43 (Ag43). Specific deletion of the *fimH* gene did not affect expression of other *fim* genes or Ag43, but did dramatically reduce the number of fimbriae expressed on the cell surface. The use of high-resolution oligonucleotide arrays for defining points of transcription initiation and termination is also demonstrated.

Communicated by W. Goebel

M.A. Schembri · H. Hasman · P. Klemm (✉)
Microbial Adhesion Group,
Section of Molecular Microbiology,
Bldg. 301, BioCentrum-DTU,
Technical University of Denmark,
DK-2800 Lyngby, Denmark
E-mail: per.klemm@biocentrum.dtu.dk
Tel.: +45-45-252506
Fax: +45-45-932809

D.W. Ussery · C. Workman
Centre for Biological Sequence Analysis,
BioCentrum-DTU,
Technical University of Denmark,
DK-2800 Lyngby, Denmark

Keywords Fimbriae · *fim* genes · Bacterial adhesins

Introduction

Bacterial adherence is normally critical for successful colonization of a specific host tissue. The best characterized group of bacterial adhesins is constituted by fimbriae (Klemm and Schembri 2000). Type 1, or mannose-sensitive, fimbriae are found on the majority of *Escherichia coli* strains and are widespread among other members of the Enterobacteriaceae (Klemm and Krogfelt 1994). The interaction between type 1 fimbriae and receptor structures has in a number of studies been shown to play a key role in the colonization of various host tissues by *E. coli* (Yamamoto et al. 1990; Bloch et al. 1992). Also, in certain strain backgrounds, type 1 fimbriae can be regarded as virulence factors. Indeed, we and others have previously shown that the expression of type 1 fimbriae in *E. coli* is linked to pathogenesis in the urinary tract (Connell et al. 1996; Mulvey et al. 1998). Type 1 fimbriae have been shown to be important for bacterial biofilm formation (Schembri and Klemm 2001) and, together with Antigen 43(Ag43), they are key determinants of the colony morphology of *E. coli* K-12 (Hasman et al. 2000).

A typical type 1 fimbriated bacterium has 200–500 peritrichously arranged fimbriae on its surface. Each organelle is a 7 nm wide, and approximately 1 μm long, rod-shaped structure. The bulk of the organelle consists of about 1000 copies of the major subunit protein, FimA, which serves as a scaffold for the receptor-recognizing adhesin FimH, which is located at the tip and perhaps also interspersed along the fimbrial shaft (Krogfelt and Klemm 1988; Krogfelt et al. 1990; Jones et al. 1995; Choudhury et al. 1999). The minor components FimF and FimG seem to act as adaptors for integration of FimH into the fimbriae (Klemm and Christiansen 1987; Jones et al. 1995). Translocation of the fimbrial components, FimA, FimF, FimG and FimH, across the inner membrane is mediated by the

normal Sec-dependent pathway. Further export to the cell exterior is dependent on a two-component system-specific transport and assembly system consisting of FimC, a chaperone located in the periplasm, and FimD, an assembly platform, or usher, present in the outer membrane. The minor components, notably FimH, have been shown to be of paramount importance for the initiation of organelle formation (reviewed by Klemm and Schembri 2000).

Expression of type 1 fimbriae is subject to phase variation, resulting in individual cells switching between a fimbriate and a non-fimbriate state. This is due to inversion of a 314-bp DNA segment located immediately upstream of the *fimA* gene. A promoter residing in this phase switch drives expression of the *fim* genes (Olsen and Klemm 1994) when the switch is in the ON orientation but not in the OFF orientation. Two recombinases, FimB and FimE, mediate inversion of the *fim* phase switch (Klemm 1986; Gally et al. 1996). Both are members of the tyrosine recombinase family (Esposito and Scocca 1997). Only the FimB recombinase efficiently promotes OFF-to-ON switching, while FimE primarily catalyses ON-to-OFF inversion (Klemm 1986; Gally et al. 1996). A number of global regulators including integration host factor (IHF) (Blomfield et al. 1997), the leucine-responsive regulatory protein (Lrp) (Blomfield et al. 1993) and H-NS (Olsen and Klemm 1994; Olsen et al. 1998; Schembri et al. 1998) also affect inversion of the *fim* switch.

DNA microarray technology permits the analysis of gene expression on a whole-genome scale. This technique has already been used successfully to study *E. coli* gene expression under a number of different growth conditions (Tao et al. 1999; Selinger et al. 2000; Wei et al. 2001). A type 1 fimbriated cell has up to 500 fimbriae on the surface, i.e, approximately half a million structural proteins, representing $\sim 8\%$ of the total cellular protein and a significant resource drain for the cell. With this in mind we have investigated whether the fimbriate state of a bacterium influences the expression of other non-related genes by inter-system crosstalk. Also, we have demonstrated the possible use of the technology to probe the individual expression levels of genes within an operon and to predict the locations of transcriptional start and stop sites.

Materials and methods

Bacterial strains and plasmids

The *E. coli* K-12 reference strain MG1655 was used in this work. Plasmids used to delete the entire *fim* gene cluster or the *fimH* gene were constructed using a two-step temperature-sensitive gene replacement system (Phillips 1999). Plasmid pMAS115 (*fim* deletion plasmid) consists of a 1.5-kb fragment from the region upstream of the *fim* locus [amplified with primers 144 (5′-GCGCGAAG CTTTAGGCGTGGCTTCCACTACG-3′) and 145 (5′-GGCCC CTGCAGCGATTTCACTATGGGTCAGG-3′)] and a 1.5-kb fragment from the region downstream of the *fim* locus [amplified with primers 178 (5′-GCGGCGGATCCCAATCGATTATTGGC GTGAC-3′) and 147 (5′-GGCCCGGATCCTGGGTGGTAT TCGGCATTGG-3′)] ligated into *Hin*dIII + *Bam*HI-digested pTSC29 (Phillips 1999). Plasmid pJKS61 (*fimH* deletion plasmid) consists of a 1.5-kb fragment from the region upstream of the *fimH* gene [amplified with primers 212 (5′-GCGCGAAGCTTGCTAT-CAGCTGAATGTCG-3′) and 213 (5′-GGCCCCTGCAGA GCAGTACAGCAAACAGG-3′)] and the 1.5-kb fragment from the region downstream of the *fimH gene* (amplified with primers 178 and 147) ligated into *Hin*dIII + *Bam*HI-digested pTSC29. These plasmids carry a temperature-sensitive origin of replication that permits them to replicate only at temperatures at or below 30°C. The plasmids were transformed into MG1655 and the recombinant strain was grown overnight at 30°C on plates supplemented with chloramphenicol (20 μg/ml). After re-growth at 30°C for 2 days, single colonies were streaked out on chloramphenicol plates and placed at 42°C to select for *recA*-mediated single crossover events. Chloramphenicol-resistant colonies were then grown at 42°C in liquid LB media containing 20 μg/ml chloramphenicol. Overnight cultures were diluted 1:1000 in liquid LB medium without antibiotics, grown to an optical density at 600 nm (OD_{600}) of 0.5, and then plated out on LB plates. Colonies from these plates were replica-plated on chloramphenicol plates and LB plates. Chloramphenicol-sensitive colonies were tested for deletion of the *fim* locus or *fimH* gene by PCR. Single colonies with deletions in the *fim* locus (MS428) and *fimH* gene (JKS132) were selected for further studies.

Plasmid pfimB (alias pPKL9) contains the *fimB* recombinase gene under transcriptional control of the tetracycline resistance gene promoter (Klemm 1986) and was used to maximise the "ON" orientation of the *fim* switch. Plasmid pMAS25 is a pBR322 derivative containing a deletion that inactivates the tetracycline resistance gene.

Microarray expression analysis

Strains were grown to late log phase ($OD_{600} = 0.9$) in LB broth at 37°C with shaking. Cells were harvested and RNA was extracted using Qiagen RNeasy columns. Enrichment of mRNA and microarray analysis was performed according to the Affymetrix Expression Analysis Technical Manual. Biotin-labelled mRNA (approximately 5 μg) was hybridised to *E. coli* GeneChip microarrays (Affymetrix, Santa Clara, Calif.) overnight at 45°C in MES buffer containing herring sperm DNA (100 μg/ml) and BSA (500 μg/ml). Washing and staining procedures were carried out as recommended using GeneChip Analysis Suite software (version 4.0). Hybridised RNA was fluorescently labelled in a three-step affinity-binding procedure that involved binding of streptavidin to biotin-labelled RNA, binding of biotin-conjugated streptavidin antibody to streptavidin, and finally binding of phycoerythrin-conjugated streptavidin to biotin-labelled antibodies. Probe arrays were scanned twice and a quantitative analysis of hybridisation patterns and intensities was performed using the GeneChip Analysis Suite software version 4.0 (Expression Analysis window).

Assessment of DNA array data

Information on probe intensity was extracted from the Affymetrix CEL files and correlated to their respective genes based on information in the *E. coli* CDF file. The PM and MM probes were normalized by the application of cubic splines as follows. The geometric mean of each PM and MM probe was calculated over the four arrays. These values defined a virtual, or centroid array and the signal distribution in each array was normalized to the distribution of the centroid. Cubic splines were fit to pairs of quantile samples, 1000 quantiles from the centroid and 1000 from each array. In this way, a cubic spline was provided for each array. Normalized array values for PM and MM were interpolated from their respective spline functions. Complete data sets were converted to colour-coded concentric wheels as previously described (Pedersen et. al. 2000).

Results

Construction of *fim*/*fimH* mutant strains

The well-characterised *E. coli* K-12 strain MG1655 contains an intact *fim* gene cluster on the chromosome. To study potential cross-talk between the *fim* system and all other genes located on the chromosome of MG1655 we constructed a set of mutants of this strain that differed in their *fim* status, namely Δ*fim*, and Δ*fimH*. To delete the entire *fim* gene cluster, a plasmid (pMAS115) was constructed. This plasmid contains PCR-amplified DNA from regions adjacent to the *fim* cluster cloned into the temperature-sensitive gene replacement plasmid pTSC29 (Phillips 1999). A double crossover and recombination event was obtained as previously described (Hasman et al. 2000). A Δ*fimH* strain was constructed in a similar manner using plasmid pJKS61. Both MG1655 and its Δ*fim* and Δ*fimH* derivatives were transformed with plasmid pfimB, encoding the *fimB* gene, to ensure optimal *fim* gene expression and to permit direct comparisons of the strains. To eliminate any possible effects of FimB that were independent of fimbrial expression we also constructed a fourth strain, by introducing a pBR322-derived vector control plasmid (pMAS125) into the Δ*fim* strain. PCR monitoring of the *fim* switch in MG1655(pfimB) and MG1655Δ*fimH*(pfimB) revealed this element to be predominantly in the ON orientation (it is absent in the other two strains).

Monitoring of gene expression within the *fim* cluster

To analyse the expression of genes in *E. coli* that might be affected by the *fim* status of the cell we used the Affymetrix DNA chip based on the *E. coli* K-12 reference strain MG1655 (Selinger et al. 2000). Total mRNA was isolated from each of the four described isogenic strains and hybridised to the oligonucleotide arrays. To view complete data sets we used our own computational tools to plot gene expression levels over the entire *E. coli* MG1655 genome in the form of colour-coded concentric wheels (Ussery et al. 2000). Figure 1 shows such an

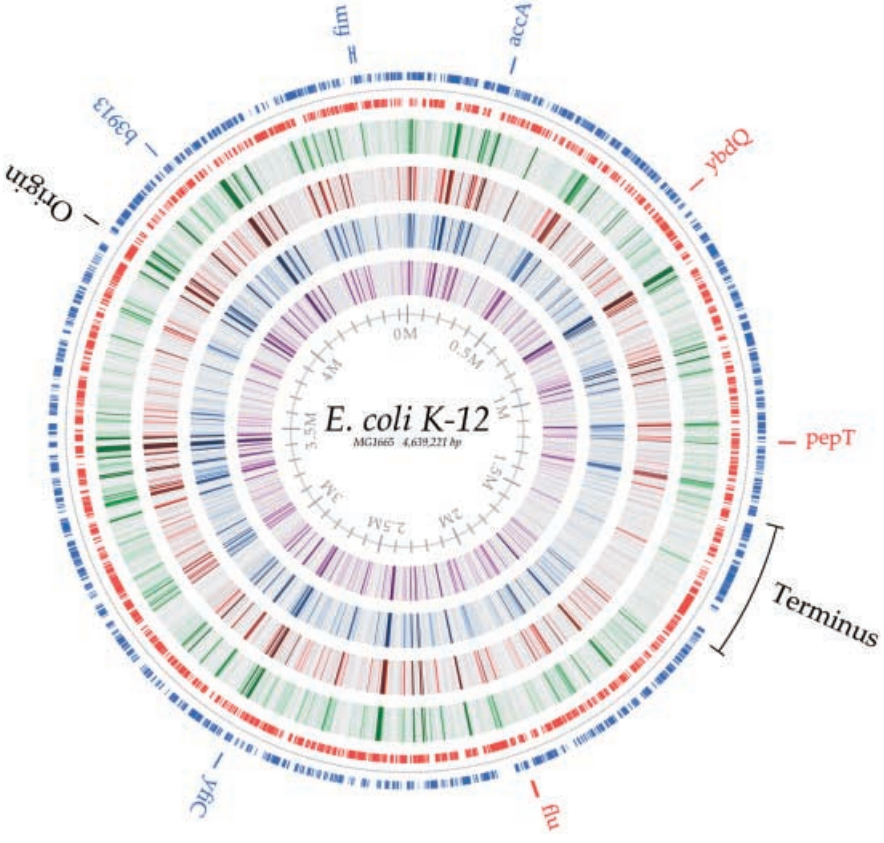

Fig. 1. DNA atlas for the entire chromosome of *E. coli* K-12 strain MG1655. The inner circles show genes expressed in MG1655 (pfimB) in *green*, MG1655Δ*fim*(pfimB) in *red*, MG1655Δ*fimH* (pfimB) in *blue*, and MG1655(pMAS125) in *purple*. The value of each measure along the DNA sequence is shown using coloured concentric wheels representing the entire chromosome as described previously (Ussery et. al. 2000). Each value is a direct representation of the quantified intensity signal obtained after scanning of the DNA array chip. Only genes differing by more than 10-fold (log scale) in expression have been indicated on the periphery (see specifically *fim* and *flu*). The reproducibility of the data is emphasized by the almost identical intensity levels for the majority of expressed genes. The numbers on the *inside* of the innermost wheel represent the position relative to 0 min measured in millions of base pairs (Mbp). The resolution of these whole-chromosome atlases is 1860 bp (i.e. the thinnest visible line in the innermost circle corresponds to a DNA region of 1860 bp). The outer circles represent coding regions on the sense (*blue*) and antisense (*red*) strands

overview for each of the four strains examined. Each coloured mark is a direct representation of the quantified signal intensity obtained after scanning of the DNA chip. This form of visual presentation gives an immediate overview of the array data and demonstrates a high level of consistency and reproducibility within the expression levels obtained.

Of specific interest to us was the ability of the array technology to quantitate differential expression of genes within the type 1 fimbrial gene cluster. Seven *fim* genes, A, I, C, D, F, G, and H, are located downstream of the switch, encoding the major structural component (A), transport machinery (C and D) and minor structural components (I, F, G, and H). The signals originating from these genes in the parent MG1655 strain indicated the following expression ratios relative to A (which was set to 100): I (28), C (8), D (9), F (4), G (10), and H (5). Almost identical values (with the exception of *fimH*) were obtained in the MG1655Δ*fimH*(pfimB) strain (Fig. 2). In order to further validate these results we made several transcriptional *fim-lacZ* reporter constructs to monitor gene expression. Fusions of *lacZ* with *fimA*, *fimI*, *fimD* and *fimH* demonstrated high expression of *fimA* with diminished activity at each subsequent downstream fusion (Fig. 3). Comparison of these results with our microarray data revealed that the data sets were in excellent agreement, and underline the reliability of the DNA array technique employed (Fig. 4). A comparison of the transcriptional activities of the *fim* genes has not been reported previously. It is therefore interesting to note that the observed transcript signals were in good agreement with our current knowledge of the composition and biogenesis of the type 1 fimbrial organelle (Klemm and Krogfelt 1994; Klemm and Schembri 2000). Furthermore, the results indicate that the primary regulation of *fim* gene product levels and consequently the stoichiometry of organelle components takes place at the transcriptional level.

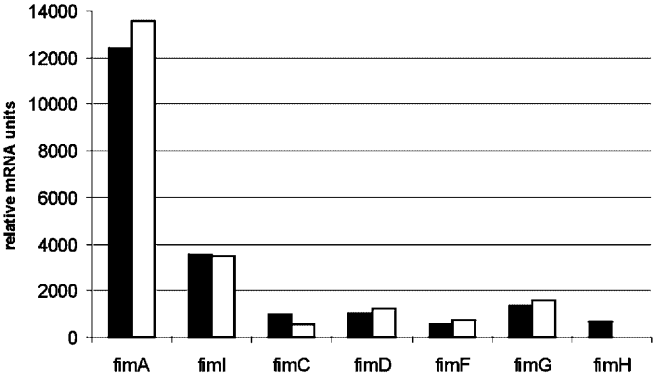

Fig. 2. Relative expression levels of each of the *fim* genes encoding structural and assembly components in MG1655(pfimB) and MG1655Δ*fimH*(pfimB)

The *fim* and *flu* genes are conversely expressed

Comparison between our fimbriate and afimbriate isogenic strains revealed that expression of the *flu* gene (encoding Ag43) was increased approximately 20-fold when *fim* was absent (Table 1). We have previously shown that fimbriae and Ag43 are phase-variable surface structures that determine colony morphology in *E. coli* K-12. Differential expression of each of these surface components gives rise to four different morphology types referred to as forms 1–4 (Hasman et al. 2000). Phase variation of type 1 fimbriae is conferred by a DNA switch, the inversion of which is controlled by two site-specific recombinases. The expression of Ag43, the product of the *flu* gene, is phase variable due to the

Fig. 3A, B. β-Galactosidase activities of transcriptional *lacZ* fusions in four *fim* genes. **A** Schematic representation of insertion points of the *lacZ* gene. **B** β-Galactosidase activities (in Miller units) of cells harbouring the corresponding plasmid shown in **A**. The *error bars* indicate the standard deviations of the means based on six measurements

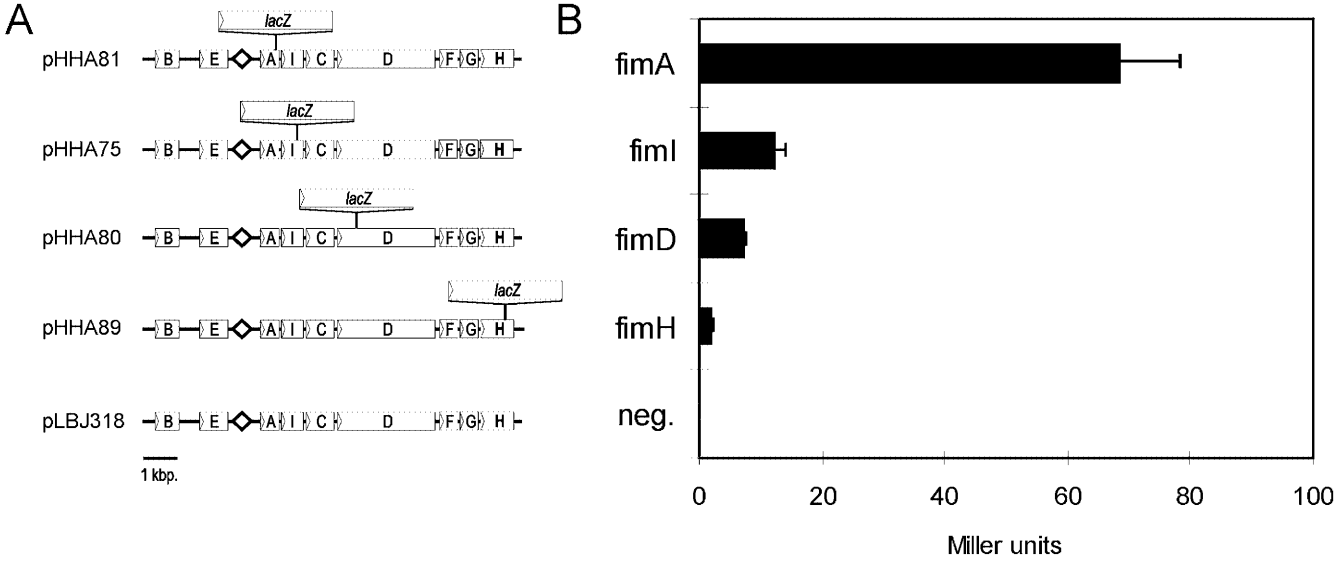

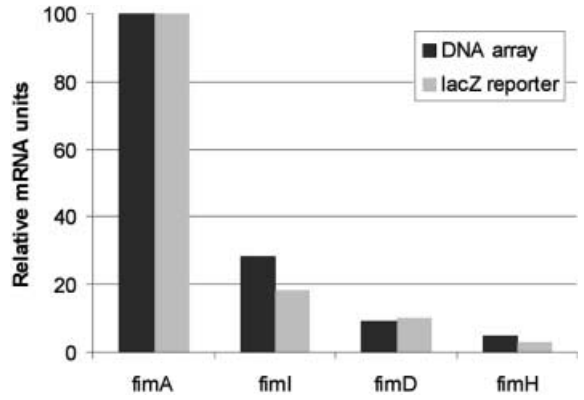

Fig. 4. Comparison between the expression levels of four *fim* genes as determined by DNA array technology and *lacZ* reporter analysis. Expression levels for *fimA* were standardized to 100 units in order to extrapolate values for *fimI*, *fimD* and *fimH*

concerted action of the Dam methylase (activation) and OxyR (repression) (Hasman et al. 1999; Henderson and Owen 1999; Haagmans and van der Woude 2000). Furthermore, we have recently demonstrated that Fim and Ag43 expression is coordinated by a signal transduction mechanism involving the thiol-disulfide status of OxyR in which fimbriation dominates (Schembri and Klemm 2001).

When the colony morphologies of the present strains were examined, MG1655(pfimB) turned out to produce characteristic small, convex, glossy colonies (form 2) that were shown to consist almost exclusively of type 1 fimbriated cells devoid of Ag43 (Fig. 5). Conversely, MG1655Δ*fim*(pfimB) produced large, flat, frizzy (form 1) colonies that consisted almost entirely of Ag43-expressing cells (Fig. 5). The array analyses indicate that the Δ*fimH* strain expresses all *fim* genes except *fimH* to the same extent as MG1655(pfimB) (Fig. 2). However, MG1655Δ*fimH* (pfimB) produced flat, irregular and smooth colonies (form 3) that consisted of cells devoid of both type 1 fimbriae and Ag43 (Fig. 5). The correlation of a bald phenotype with a Δ*fimH* genotype has previously been reported (Schembri et al. 1996) and is consistent with our current model of fimbrial biogenesis, which depicts FimH as an initiator of organelle synthesis (Choudhury et al. 1999). Finally, most of the colonies from our control strain MG1655Δ*fim*(pMAS125) were of form 1 type with Ag43-expressing cells (Fig. 5).

Use of expression data to map transcription start and stop sites

The *E. coli* K-12 Affymetrix array contains on average one 25mer oligonucleotide probe per 30 bp over the entire genome (Selinger et al. 2000). Based on this information, we hypothesized that the hybridisation signals within intergenic regions could be used to map promoters and transcriptional start and stop sites over the entire genome. As an example we chose to examine the region upstream of the *flu* coding sequence, the promoter of which has not previously been mapped. Moving upstream from the *flu* gene we scanned the hybridisation intensities from our array data and found that the probe covering nucleotides 2069339–2069363 was the last to give a positive signal (Fig. 6).

Table 1. Relative changes in expression levels of genes altered with respect to those in MG1655(pfimB) cells

Gene/b-number	MG1655Δ*fim* (pfimB)[a,b]	MG1655Δ*fimH* (pfimB)[a]	Functional group	Gene product
Down-regulated genes				
accA	–16.2	–19.5	Fatty acid and phospholipid metabolism	AcetylCoA carboxylase
b3913	–10.0	–2.8	Unclassified	Putative periplasmic protein
fimA	–169.7	1.1	Surface structures	Major type 1 fimbrial subunit
fimC	–20.2	–1.6	Surface structures	Type 1 fimbrial chaperone protein
fimD	–18.1	1.1	Surface structures	Type 1 fimbrial usher protein
fimF	–11.9	1.4	Surface structures	Minor type 1 fimbrial subunit
fimG	–22.4	1.2	Surface structures	Minor type 1 fimbrial subunit
fimH	–16.3	–14.0	Surface structures	Type 1 fimbrial adhesin
fimI	–74.9	–1.1	Surface structures	Type 1 fimbrial subunit protein
yfiC	–10.0	–1.9	Putative enzymes	Putative enzyme
Up-regulated genes				
flu	19.6	1.1	Cell structure	Outer membrane fluffing protein
pepT	11.2	9.8	Cell structure	Putative peptidase T
ybdQ	2.9	21.6	Unclassified	Putative filament protein

[a]Analysis of data was performed with the Affymetrix MicroSuite 4.0 software. Genes were considered to be altered in expression if in at least one of the strains examined they were: (1) identified as present (i.e. absolute call), (2) yielded an average difference call of greater than 1000 (i.e. average probe hybridisation intensity value) and (3) displayed a relative difference of greater than tenfold. The data shown are relative changes as calculated by the Affymetrix MicroSuite 4.0 software

[b]Gene expression levels in MG1655Δ*fim*(pMAS125) were essentially the same as in MG1655Δ*fim*(pfimB)

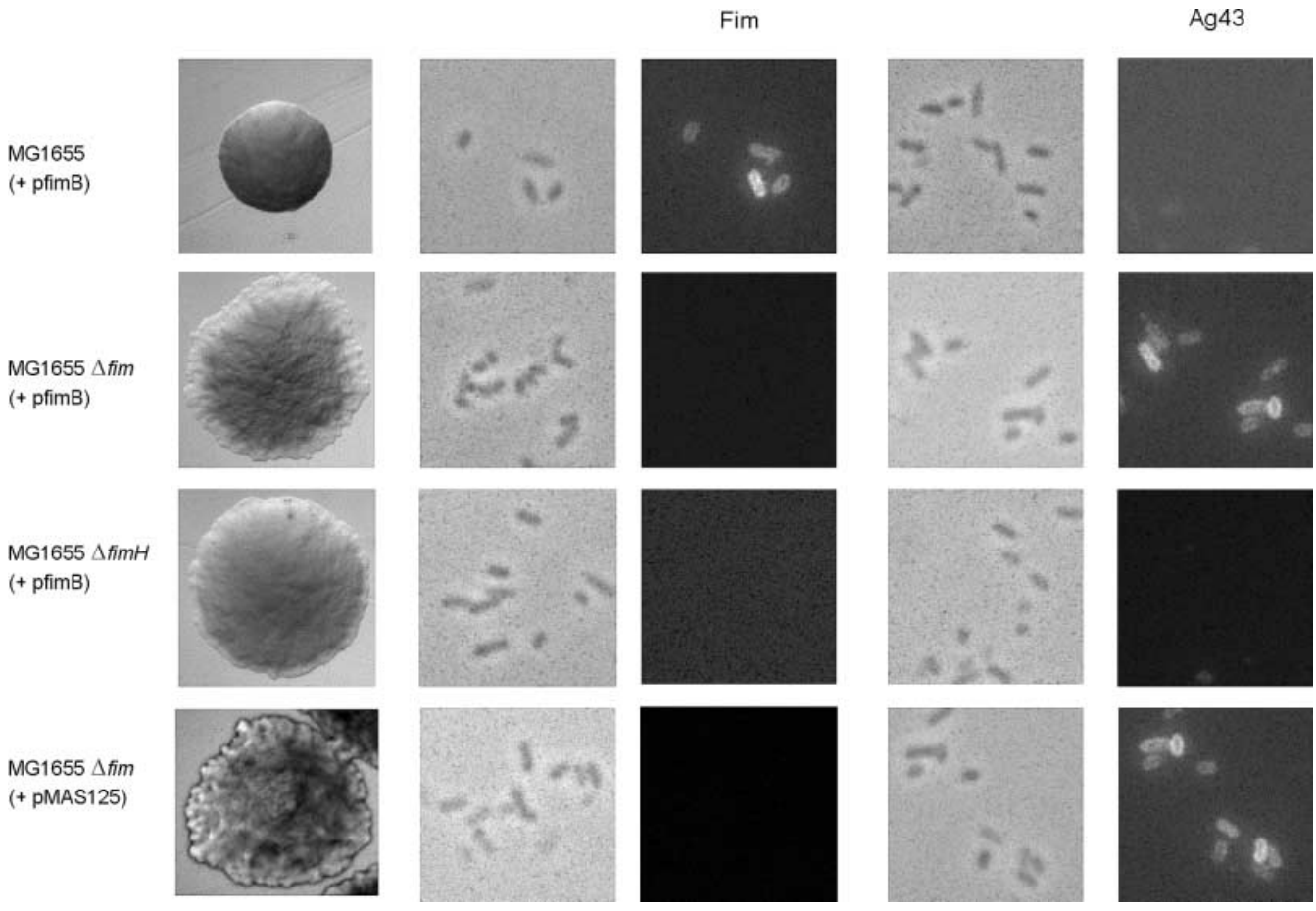

Fig. 5. Phase-contrast microscopy of colonies (*leftmost column*) and subsequent phase-contrast and immunofluorescence microscopy of cells of *E. coli* strains MG1655(pfimB), MG1655Δ*fim*(pfimB), MG1655Δ*fimH*(pfimB) and MG1655(pMAS125) employing anti-Fim and anti-Ag43 serum, respectively

Examination of the sequence immediately upstream of this probe revealed a likely $\sigma 70$ promoter consensus sequence TTGTCC–17 bp–TAGAAT (Fig. 6A) and actually confirms our previous predictions (Hasman et al. 1999). We were also able to map the termination of transcription to a region of dyad symmetry immediately downstream of the *flu* gene (Fig. 6B). Taken together, the analysis indicates the potential use of this kind of microarray for mapping transcription initiation and termination sites on a whole-genome level.

Other genes affected by *fim* status

Comparison of global gene expression within each of the four strains revealed few differences apart from *flu* (Fig. 1 and Table 1). Here we decided to focus specifically on the MG1655Δ*fimH* (pfimB) strain. While the *fimH* mutation had no direct effect on the transcription of other upstream *fim* genes, it did result in a dramatic reduction in the number of fimbriae produced on the bacterial surface (Fig. 5). This observation has also been reported previously and is most likely to be due to the role of FimH as an initiator of fimbrial biogenesis through donor-strand complementation (Klemm et al. 1994; Schembri et al. 1996; Choudhury et al. 1999).

We hypothesized that the alterations in gene expression in the MG1655Δ*fimH* (pfimB) strain might be the result of a signalling mechanism activated by the accumulation of fimbrial proteins in the periplasm that cannot be channelled effectively into organelle synthesis due to the lack of FimH initiator protein. In the related P fimbrial system, accumulation of misfolded proteins in the periplasm results in the activation of the Cpx two-component signal transduction system that controls a stress response (Hung et al. 2001). Phosphorylated CpxR binds to a specific DNA sequence within the *pap* promoter and up-regulates factors that facilitate pilus assembly. A potential Cpx consensus-binding site is located proximal to the type 1 fimbrial promoter and within the switch. However, our array data did not reveal any difference in *cpx* gene expression in MG 1655Δ*fimH*(pfimB). Furthermore, transcription of genes encoding periplasmic factors known to be affected by the Cpx two-component system, such as *nlpE*, *degP*, *dsbA* and *ppiA*, were also unaffected. We also examined type 1 fimbrial gene expression in a *cpx* mutant background but observed no effect. Therefore, it appears that signal transduction mechanisms related to type 1 fimbrial

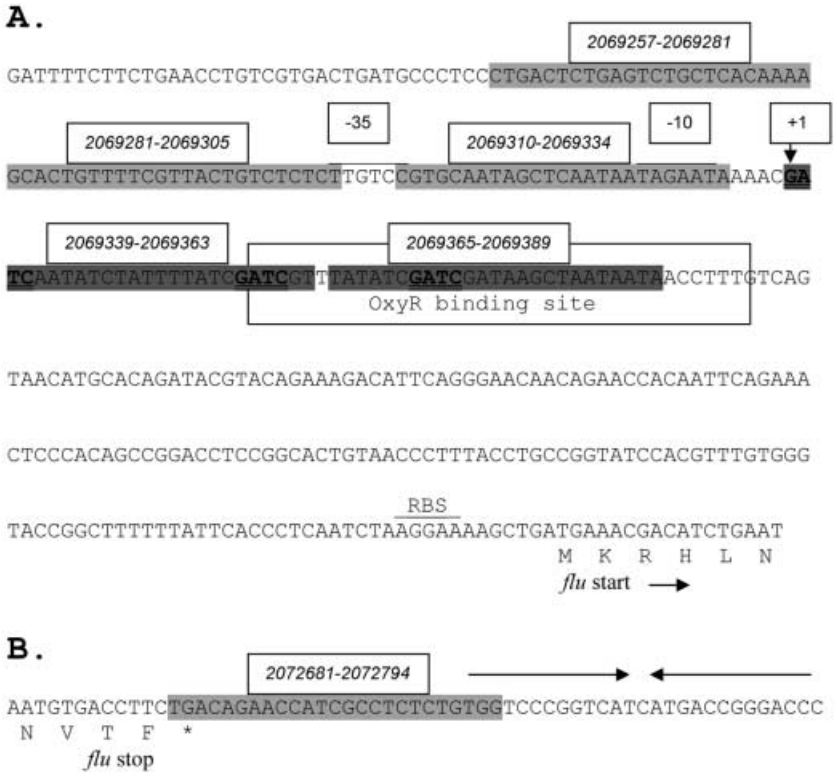

Fig. 6A Nucleotide sequence of the 5′ region of the *flu* gene. Positions of the probe oligonucleotides on the Affymetrix DNA chip are indicated. Positive (hybridising) probes are shaded *dark grey* and negative (non-hybridising) probes are shaded *light grey*. The promoter sequence and transcription start site are indicated. Also shown are the OxyR binding site, predicted GATC Dam methylation sites (in *bold face* and *double underlined*), ribosome binding site (RBS) and the beginning of the coding region of the *flu* gene. **B** Nucleotide sequence of the 3′ region of the *flu* gene. The negative hybridisation probe is shaded *light grey* and the predicted transcription termination loop is indicated

biosynthesis are different to those observed with P pili. At this stage it is not possible to determine if the accumulation of unincorporated type 1 fimbrial products directly affects global gene expression.

Discussion

In nature most bacteria attach to, and live in close association with, surfaces. Indeed, the first important step in the establishment of sessile bacterial communities or biofilms is adhesion – often conferred by specific bacterial adhesins. Such adhesins exhibit exquisite selectivity for target molecules and recognize molecular motifs in a lock-and-key fashion. Specific adhesion allows targeting of a given bacterium to a specific surface, and expression of a given adhesin acts as an address indicator for the microbe. Elaboration of an adhesin at a given time and place is crucial in determining the fate of a bacterium in the environment, and most often heralds a shift from a planktonic to a sessile lifestyle. Type 1 fimbriae are mannose-sensitive adhesive organelles that mediate binding to the TM4 family of proteins (uroplakin Ia and Ib) in the bladder epithelium via the FimH adhesin (Wu and Sun 1993; Pak et al 2001). FimH-mediated binding to other targets, such as CD48 on mast cells (Malaviya et al. 1999), laminin (Kukkonen et al 1993), collagen (Pouttu et al. 1999), fibronectin (Sokurenko et al 1992; Schembri et al. 2000) and abiotic surfaces (Pratt et al. 1998; Schembri and Klemm 2001), has also been reported. While the mechanisms of fimbrial biogenesis are now better understood, the molecular events involved in response to fimbrial gene expression remain unknown. Against this background we have investigated the effects of mutations in the *fim* genes in *E. coli* by using DNA arrays to scan the transcriptional profile of the entire genome.

The Affymetrix *E. coli* genome array employs oligonucleotide probes in a high-resolution capacity that permits one to define operon structures. We have specifically applied this feature to study the type 1 fimbrial gene operon. Our data support the notion that a single promoter located in the switch segment drives the expression of all genes downstream of this element. We observed significant reductions in expression levels going from *fimA* to *fimH*. This suggests that the primary regulation of Fim stoichiometry takes place at the transcriptional level. However, our current knowledge of organelle structure and composition indicates that post-transcriptional factors, such as modulation by different ribosomal binding sites, probably contribute to the fine-tuning of the organelle stoichiometry. The expression data also points to the existence of a transcription attenuator immediately after *fimA*. A region of dyad symmetry is located 31 bp downstream of the *fimA* gene and probe hybridisation intensities on the array localise the transcriptional attenuation to this region. A similar pattern of transcription attenuation is also observed after the gene encoding the major subunit of P fimbriae (*papA*) in the corresponding operon (Naureckiene and Uhlin 1996).

The global gene expression profiles for each of the isogenic strains we examined were extremely similar. Therefore, it seems that, despite the considerable

metabolic demands that are arguably associated with fimbrial biogenesis, gene expression was largely unaltered under the growth conditions employed. The most prominent difference in gene expression between fimbriate and non-fimbriate cells involved the Ag43-encoding *flu* gene, the expression of which was coordinated oppositely to that of the *fim* genes. These observations were supported by examination of the colony morphology of each strain and were subsequently confirmed by immunofluorescence microscopy employing Ag43- and FimA-specific antisera. Ag43 synthesis is repressed by the reduced form of OxyR, a global regulator that monitors the thiol disulfide status of the cell (Storz and Imlay 1999). The biosynthesis of fimbriae, which is directly associated with massive disulfide bridge formation, constitutes a signal transduction mechanism that represses the expression of the *flu* gene via the thiol-disulfide status of OxyR (Schembri and Klemm 2001). Based on this model, OxyR should be predominantly in the reduced form in the MG1655(pfimB) strain. We did not identify any other genes that displayed similar regulatory characteristics to the *flu* gene.

The MG1655Δ*fimH* (pfimB) strain was severely affected in its ability to synthesize intact fimbrial organelles on the cell surface, despite the fact that the expression of all other genes in the type 1 fimbrial operon was unaffected. These observations are consistent with the notion that FimH plays a key role in the initiation of fimbrial biogenesis. Expression data and immunofluorescence microscopy demonstrated that the synthesis of Ag43 was also dramatically reduced in this strain. Therefore, it seems that fimbriae-induced signal transduction via OxyR also takes place when the structural components are made and presumably accumulate in the periplasm, even though virtually no fimbriae are produced.

An additional application associated with the *E. coli* genome array used here involves the ability to map transcriptional start and stop sites. To illustrate this aspect we mapped the promoter of the *flu* gene. Consistent positive hybridisation signals were obtained up to 162 bp from the previously identified ATG translation start site. This type of application is only possible with high-resolution oligonucleotide arrays. We are currently examining all intergenic regions covered by the probes on the array to map transcriptional starts and stops over the entire genome.

Contact between bacterial adhesins and their complementary receptors on host cells is a dynamic event that can trigger responses in host cells as well as in bacteria. We are currently examining global gene and protein expression patterns in response to adhesion to both living and inert surfaces. It is likely that molecular cross-talk mechanisms will be identified that are associated with adhesion to specific targets in different environments. It may even be possible to define specific gene expression profiles for adhered bacteria in different ecological niches. Such knowledge may identify new genes associated with bacterial adhesion mechanisms, the products of which may form a collection of new targets for novel drugs.

Acknowledgements This work is supported by the Danish Medical Research Council (Grant No. 9802358) and the Danish Natural Sciences Research Council (Grant No. 51-00-0291). MAS is supported by a Skou stipend from the Danish Natural Sciences Research Council (Grant No. 21-01-0296). DU and CW are funded by a grant from the Danish Research Foundation to Søren Brunak.

References

Bloch CA, Stocker BAD, Orndorff PE (1992) A key role for type 1 pili in enterobacterial communicability. Mol Microbiol 6:697–701

Blomfield IC, Calie PJ, Eberhardt KJ, McClain MS, Eisenstein BI (1993) Lrp stimulates phase variation of type 1 fimbriation in *Escherichia coli* K-12. J Bacteriol 175:27–36

Blomfield IC, Kulasekara DH, Eisenstein BI (1997) Integration host factor stimulates both FimB- and FimE-mediated site-specific DNA inversion that controls phase variation of type 1 fimbriae expression in *Escherichia coli*. Mol Microbiol 23:705–717

Choudhury D, Thompson A, Stojanoff V, Langermann S, Pinkner J, Hultgren SJ, Knight SD (1999) X-ray structure of the FimC-FimH chaperone-adhesin complex from uropathogenic *Escherichia coli*. Science 285:1061–1066

Connell H, Agace W, Hedlund M, Klemm P, Schembri M, Svanborg C (1996) Type 1 fimbrial expression enhances *Escherichia coli* virulence for the urinary tract. Proc Natl Acad Sci USA 93:9827–9832

Esposito D, Scocca JJ (1997) The integrase family of tyrosine recombinases: evolution of a conserved active site domain. Nucleic Acids Res 25:3605–3614

Gally DL, Leathart J, Blomfield IC (1996) Interaction of FimB and FimE with the *fim* switch that controls the phase variation of type 1 fimbriae in *Escherichia coli* K-12. Mol Microbiol 21:725–738

Haagmans W, van der Woude M. (2000) Phase variation of Ag43 in *Escherichia coli*: Dam-dependent methylation abrogates OxyR binding and OxyR-mediated repression of transcription. Mol Microbiol 35:877–887

Hasman H, Chakraborty T, Klemm P (1999) Antigen 43-mediated autoaggregation is blocked by fimbriation. J Bacteriol 181:4834–4841

Hasman H., Schembri MA, Klemm P (2000) Antigen 43 and type 1 fimbriae determine colony morphology of *Escherichia coli* K-12. J Bacteriol 182:1089–1095

Henderson IR, Owen P (1999) The major phase-variable outer membrane protein of *Escherichia coli* structurally resembles the immunoglobulin A1 protease class of exported proteins and is regulated by a novel mechanism involving Dam and OxyR. J Bacteriol 181:2132–2141

Hung DL, Raivio TL, Jones CH, Silhavy TJ, Hultgren SJ (2001) Cpx signaling pathway monitors biogenesis and affects assembly and expression of P pili. EMBO J 20:1508–1518

Jones CH, Pinkner JS, Roth R, Heuser J, Nicholes AV, Abraham SN, Hultgren SJ (1995) FimH adhesin of type 1 pili is assembled into a fibrillar tip structure in the *Enterobacteriaceae*. Proc Natl Acad Sci USA 92:2081–2085

Klemm P (1986) Two regulatory *fim* genes, *fimB* and *fimE*, control the phase variation of type 1 fimbriae in *Escherichia coli*. EMBO J 5:1389–1393

Klemm P, Christiansen G (1987) Three *fim* genes required for the regulation of length and mediation of adhesion of *Escherichia coli* type 1 fimbriae. Mol Gen Genet 208:439–445

Klemm P, Krogfelt KA (1994) Type 1 fimbriae of *Escherichia coli*. In: Klemm P (ed) Fimbriae: adhesion, genetics, biogenesis and vaccines. CRC Press, Boca Raton, pp 9–26

Klemm P, Schembri MA (2000) Bacterial adhesins: structure and function. Int J Med Microbiol 290:27–35

Klemm P, Christiansen G, Kreft B, Marre R, Bergmans H (1994) Reciprocal exchange of minor components of type-1 and F1C fimbriae results in hybrid organelles with changed receptor specificities. J Bacteriol 176:2227–2234

Krogfelt KA, Klemm P (1988) Investigation of minor components of *Escherichia coli* type 1 fimbriae: protein chemical and immunological aspects. Microb Pathog 4:231–238

Krogfelt KA, Bergmans H, Klemm P (1990) Direct evidence that the FimH protein is the mannose-specific adhesin of *Escherichia coli* type 1 fimbriae. Infect Immun 58:1995–1998

Kukkonen M, Raunio T, Virkola R, Lahteenmaki K, Makela PH, Klemm P, Clegg S, Korhonen TK (1993) Basement membrane carbohydrate as a target for bacterial adhesion: binding of type I fimbriae of *Salmonella enterica* and *Escherichia coli* to laminin. Mol Microbiol 7:229–237

Malaviya R, Gaol Z, Thankavel K, van der Merwe PA, Abraham SN (1999) The mast cell tumor necrosis factor alpha response to FimH-expressing *Escherichia coli* is mediated by the glycosylphosphatidylinositol-anchored molecule CD48. Proc Natl Acad Sci USA 96:8110–8115

Mulvey MA, Lopez-Boado YS, Wilson CL, Roth R, Parks WC, Heuser J, Hultgren SJ (1998) Induction and evasion of host defenses by type 1-piliated uropathogenic *Escherichia coli*. Science 282:1494–1497

Naureckiene S, Uhlin BE (1996) In vitro analysis of mRNA processing by RNase E in the *pap* operon of *Escherichia coli*. Mol Microbiol 21:55–68

Olsen PB, Klemm P (1994) Localization of promoters in the *fim* gene cluster and the effect of H-NS on the transcription of *fimB* and *fimE*. FEMS Microbiol Lett 116:95–100

Olsen PB, Schembri MA, Gally DL, Klemm P (1998) Differential temperature modulation by H-NS of the *fimB* and *fimE* recombinase genes which control the orientation of the type 1 fimbrial phase switch. FEMS Microbiol Lett 162:17–23

Pak J, Pu Y, Zhang ZT, Hasty DL, Wu XR (2001) Tamm-Horsfall protein binds to type 1 fimbriated *Escherichia coli* and prevents *E. coli* from binding to uroplakin Ia and Ib receptors. J Biol Chem 276:9924–9930

Pedersen AG, Jensen LJ, Brunak S, Staerfeldt HH, Ussery DW (2000) A DNA structural atlas for *Escherichia coli*. J Mol Biol 299:907–930

Phillips GJ (1999) New cloning vectors with temperature-sensitive replication. Plasmid 41:78–81

Pouttu R, Puustinen T, Virkola R, Hacker J, Klemm P, Korhonen TK (1999) Amino acid residue Ala-62 in the FimH fimbrial adhesin is critical for the adhesiveness of meningitis-associated *Escherichia coli* to collagens. Mol Microbiol 31:1747–1757

Pratt LA, Kolter R (1998) Genetic analysis of *Escherichia coli* biofilm formation: roles of flagella, motility, chemotaxis and type I pili. Mol Microbiol 30:285–93

Schembri MA, Klemm P (2001) Coordinate gene regulation by fimbriae-induced signal transduction. EMBO J 20:3074–3081

Schembri MA, Pallesen L, Connell H, Hasty DL, Klemm P (1996) Linker insertion analysis of the FimH adhesin of type 1 fimbriae in an *Escherichia coli fimH*-null background. FEMS Microbiol Lett 137:257–263

Schembri MA, Olsen PB, Klemm P (1998) Orientation-dependent enhancement by H-NS of the activity of the type 1 fimbrial phase switch promoter in *Escherichia coli*. Mol Gen Genet 259:336–344

Schembri MA, Sokurenko EV, Klemm P (2000) Functional flexibility of the FimH adhesin: insights from a random mutant library. Infect Immun 68:2638–46

Selinger DW, Cheung KJ, Mei R, Johansson EM, Richmond CS, Blattner FR, Lockhart DJ, Church GM (2000) RNA expression analysis using a 30 base pair resolution *Escherichia coli* genome array. Nat Biotechnol 18:1262–1268

Sokurenko EV, Courtney HS, Abraham SN, Klemm P, Hasty DL (1992) Functional heterogeneity of type 1 fimbriae of *Escherichia coli*. Infect Immun 60:4709–4719

Storz G, Imlay JA (1999) Oxidative stress. Curr Opin Microbiol 2:188–194

Tao H, Bausch C, Richmond C, Blattner FR, Conway T (1999) Functional genomics: expression analysis of *Escherichia coli* growing on minimal and rich media. J Bacteriol 181:6425–6440

Ussery D, Larsen TS, Wilkes KT, Friis C, Worning P, Krogh A, Brunak S (2001) Genome organisation and chromatin structure in *Escherichia coli*. Biochimie 83:201–212

Wei Y, Lee JM, Richmond C, Blattner FR, Rafalski JA, LaRossa RA (2001) High-density microarray-mediated gene expression profiling of *Escherichia coli*. J Bacteriol 183:545–556

Wu X-R, Sun T-T (1993) Molecular cloning of a 47 kDa tissue-specific and differentiation-dependent urothelial cell surface glycoprotein. J Cell Sci 106:31–43

Yamamoto T, Fujita K, Yokota T (1990) Adherence characteristics to human intestinal mucosa of *Escherichia coli* isolated from patients with diarrhoea or urinary tract infections. J Infect Dis 162:896–908